Journal of Thermal Analysis and Calorimetry, Vol. 78 (2004) 113–124

CURE BEHAVIOR OF EPOXY RESIN/MMT/DETA NANOCOMPOSITE
Resin curemeter

W. B. Xu [1,3]* *Z. F. Zhou* [1], *P. S. He* [2] *and W.-P. Pan* [3]

[1]Department of Polymer Science and Engineering, Hefei University of Technology, Hefei 230009, Anhui, China
[2]Department of Polymer Science and Engineering, University of Science and Technology of China, Hefei 230026, Anhui, China
[3]Department of Chemistry, Materials Characterization Center, Western Kentucky University, Bowling Green, KY, 42101, USA

Abstract

The Flory's gelation theory, non-equilibrium thermodynamic fluctuation theory and Avrami equation have been used to predict the gel time t_g and the cure behavior of epoxy resin/organo-montmorillonite/diethylenetriamine intercalated nanocomposites at various temperatures and organo-montmorillonite loadings. The theoretical prediction is in good agreement with the experimental results obtained by dynamic torsional vibration method, and the results show that the addition of organo-montmorillonite reduces the gelation time t_g and increases the rate of curing reaction, the value of k, and half-time of cure after gelation point $t_{1/2}$ decreases with the increasing of cure temperature, and the value of n is ~2 at the lower temperatures (<60°C) and decreases to ~1.5 as the temperature increases, and the addition of organo-montmorillonite decreases the apparent activation energy of the cure reaction before gelation point, but has no apparent effect on the apparent activation energy of the cure reaction after gelation point. There is no special curing process required for the formation of epoxy resin/organo-montmorillonite/diethylenetriamine intercalated nanocomposite.

Keywords: Avrami equation, cure, diethylenetriamine, epoxy resin, gel time, montmorillonite, nanocomposite, non-equilibrium thermodynamic fluctuation theory

Introduction

Nanoscale dispersion of polymer composite, which dispersed on a nanometer scale, is called to be nanocomposite. One approach to such nanocomposites, is in situ polymerization via polymer-layered silicates [1, 2]. In general, the dispersion of clay particles in a polymer matrix can result in the formation of three general types of composite materials: conventional composites, intercalated composites, and exfoliated composites. Intercalated composites are formed by the insertion of polymer chains into the clay host galleries raising the basal spacing, but the regular clay gallery structure retains its integrity. Exfoliated nanocomposites are the result of the individual 10 Å thick silicate layers being dispersed in the polymer matrix noted by the destruction of the gallery structure as the silicate layers are completely segregated from one another.

---

* Author for correspondence: E-mail: wbxu@ustc.edu

1388–6150/2004/ $ 20.00

Akadémiai Kiadó, Budapest
Kluwer Academic Publishers, Dordrecht

Recently, great attention has been paid to the layer silicate–epoxy nanocomposites. The influence of the nature of clay [3], and the structure of cure agent [4], as well as its concentration [5] on the formation of exfoliated nanocomposites have been examined with efforts. Giannelis [6] prepared exfoliated layer silicate–epoxy nanocomposites from the diglycidyl ether of bisphenol-A and nadic methyl anhydride as curing agents, and found that the dynamic storage modulus of the nanocomposites containing 4 vol% silicate was approximately 58% higher in the glassy region and 450% higher in the rubbery plateau region compared to the pristine polymer. Monolithic epoxy exfoliated-clay nanocomposites have been prepared from the reaction of alkylammonium-exchanged smectite clays with diglycidyl ether of bisphenol A and *m*-phenylenediamine as the curing agent by Pinnavaia and his coworkers [7–9]. They found that monolithic exfoliated clay nanocomposites could be formed by preswelling alkylammonium ion exchanged forms of the clays with epoxy resin prior to curing, and dramatic improvement in the tensile strength and modulus was realized, particularly when the matrix exhibited a subambient glass transition temperature. For instance, the reinforcement provided by the silicate layers at 16 mass% loading was manifested by more than 10-fold improvements in both tensile strength and modulus. However, few reports are found on the cure process by in situ nanocomposite formation.

The cure process of the epoxy–clay system is the crosslinking of linear macromolecules with a very complicated mechanism. As soon as the crosslinkings form, the resin will not be solved and melted, which leads quite a bit of difficulty to study. Traditionally, chemical analysis, IR [10], and calorimetry [11, 12] detecting the degree of conversion of reactive groups were used to study the cure process. However, the increasing consumption of reactive groups is already not obvious at the last curing stage and the sensitivity and function of these analysis techniques will be reduced significantly. But the cure process can be studied successfully with mechanical methods, and the dynamic torsional vibration method developed in our lab has successfully been used to investigate the cure behavior of epoxy resin–BF_3–MEA system and epoxy resin–triethanolamine system [13, 14].

In this presentation, the intercalated nanocomposite was prepared via mixing epoxy resin with the desired amount of clay exchanged with alkylammonium bromide and with diethylenetriamine as the curing agent. The isothermal cure process was investigated in situ by the dynamic torsional vibration method, and the non-equilibrium thermodynamic fluctuation theory and Avrami equation are used to analyze and predict the cure behavior of epoxy resin/Org-MMT/diethylenetriamine nanocomposite.

Experimental

Materials

Na^+-montmorillonite, the cation exchange capacity (CEC) value of which is about 100 mmol/100 g, was purchased from Qingshan Chemistry Agent Factory in Lin'an, China. The diglycidyl ether of biphenyl A, epoxy resin E-51 with the epoxy value 0.48–0.54 and average epoxy equivalent 196, was obtained from Shanghai resin factory. Diethylenetriamine (DETA) was used as the curing agent. $(CH_3)_3(CH_2)_{15}NBr$, the surfactant of clay, was purchased from the Research Institute of Xinhua active material in Changzhou, and preparation of organo-montmorillonite (Org-MMT) by ion exchange was carried out according to previously reported methods [15]. For the isothermal cure experiment, the epoxy resin and the curing agent are mixed in the stoichiometric ratio of 100 parts resin to 12 parts curing agent (by mass). Then the mixture is mixed with Org-MMT powder with loadings of 0, 5 and 10 parts per hundred resin (phr), respectively.

Experimental curve analysis

Dynamic torsional vibration is a non-resonant forced vibration. The schematic diagram of a homemade experimental setup of the dynamic torsional vibration was shown in Fig. 1, and the monitor of the apparatus and the information for the cure process is collected by a computer. The experimental cure obtained by dynamic torsional vibration apparatus is shown in Fig. 2. The abscissa is the curing time and the ordinate is the torque required to turn the resin system by a small angle, which corresponds to the modulus and viscosity of the resin system, and can be thought of as a relative parameter of the degree of cure. The time of closure of the molds is taken as the starting time of cure, that is, the original point O. In the range OA of the curing time the network structure formed during the cure reaction is not enough to cause forced vibration of the upper mold. As a result, the strain gauge load cell will not have any signal, so that the experimental cure is a linear line corresponding to the abscissa. At point A, the viscosity of resin system is high enough (i.e., the network formed is completed enough) for the gelation in the resin system to occur, and the torque appears and strain gauge load cell inputs signal. Thus, the point A is the gel point and the time corresponding to OA is the gel time t_g for the system. After point A the torque increases with increasing of the curing time. The increasing amplitude of the torque (slope of the curve) expresses the rate of curing reaction. The increasing trend of the torque tended to steady with increasing curing time, and the equilibrium torque G_∞ is reached at point B. The curing reaction is completed and a cup-like experimental cure is obtained. The time corresponding to OC is the full curing time and

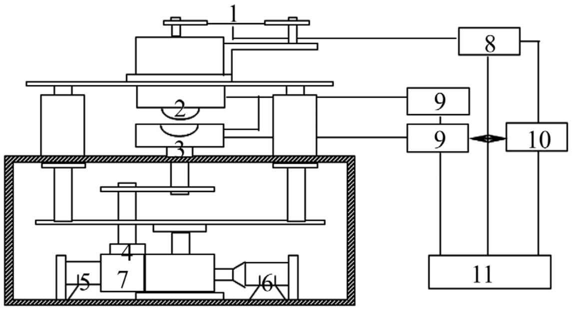

Fig. 1 Schematic representation of HLX-1 type dynamic torsional vibration apparatus

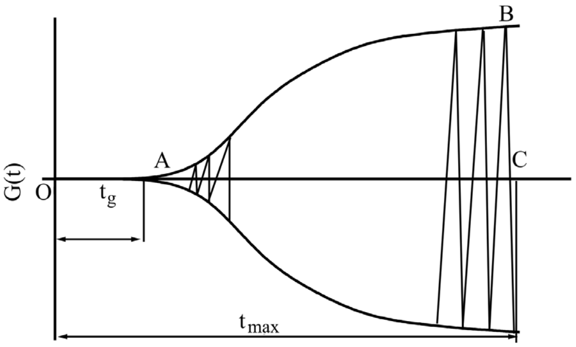

Fig. 2 Schematic representation of isothermal cure curve by dynamic torsional vibration method

the maximum equilibrium torque BC can be thought of as a relative degree of cure for the system. The envelope of the experimental cure corresponds to the change of mechanical behavior of the resin system during cure and represents the isothermal cure curve of the resin system, and the system time error of HLX-1 type dynamic torsional vibration apparatus is 2 s.

Measurement and characterization

The change of lattice spacing of montmorillonite was measured by using a Rigaku D/max-γB rotating anode X-ray diffractometer with the CuK_α line (λ=1.5418 Å), a tube voltage of 40 kV and tube current of 100 mA. The scanning range is from 1.2 to 10° with a rate of 1° min^{-1}.

Results and discussion

X-ray diffraction analysis

XRD patterns for epoxy resin/clay/diethylenetriamine composite containing different content of organoclay cured under the temperature of 70°C are shown in Fig. 3. These XRD patterns reveal the change in clay basal spacing that occurs in the epoxy curing process. For the epoxy resin/Org-MMT/diethylenetriamine system, it is noteworthy that the (001) peak, responding to the basal spacing of montmorillonite, shifted to the low angle comparable to that of the Org-MMT, and the intensity of peak increased with increasing the content of organophilic montmorillonite. For Org-MMT, the X-ray diffraction peak occurs in the site of $2\theta=4.22°$. For the epoxy resin/Org-MMT/diethylenetriamine composite, the first peak (n=1) and the second peak (n=2) of diffraction appeared at $2\theta=2.44°$, $2\theta=5.05°$ respectively, and the lattice spacing of different diffraction layer can be calculated according to Bragg equation, $2d\sin\theta=n\lambda$. Obviously, the intercalated nanocomposite with the lattice spacing of 36.2 Å was obtained. As Pinnavaia [9] pointed out that the lattice spacing of intercalated nanocomposite increases, with increased Org-MMT loading as shown by the shift to lower angles of the

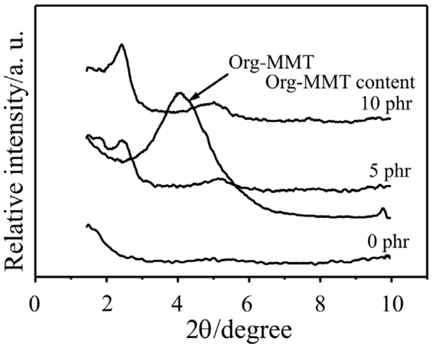

Fig. 3 XRD patterns of epoxy resin/Org-MMT/DETA systems

diffraction peak. If the lattice spacing continues to increase, exfoliated nanocomposite is formed, leading to disappearance of Bragg diffraction.

Isothermal cure curve of epoxy resin/Org-MMT/diethylenetriamine

Figure 4 is the isothermal cure curves of the epoxy/diethylenetriamine/Org-MMT complex with various Org-MMT contents at 40, 50, 60 and 70°C, respectively. The cure curves at different temperatures have a similar shape, but obvious differences in their gel times and rates of cure reaction. It is evident from Fig. 4 that with the increasing cure temperature the gel time decreases in turn, and the rate of cure reaction becomes more rapid. The gel time t_g obtained from Fig. 4 and some related data are listed in Table 1.

Theoretical prediction of cure behavior

Hsich's nonequilibrium thermodynamic fluctuation theory [16, 17] directly describes the changes of physical or mechanical properties of a system during cure. According

Table 1 Isothermal cure data of Epoxy/Org-MMT/DETA at different temperature

Org-MMT (phr)	T/°C	t_g/min	t/min	β	ΔH/kJ mol^{-1}
0	40	40.01	11.84	1.88	44.0
	50	19.83	9.72	2.53	
	60	11.93	6.60	1.50	
	70	3.01	3.03	1.72	
5	40	37.65	13.35	3.09	40.3
	50	19.52	9.18	2.48	
	60	10.73	4.63	1.78	
	70	4.95	3.71	1.16	
10	40	38.70	12.74	4.02	44.7
	50	19.04	9.86	4.34	
	60	10.91	6.50	1.56	
	70	4.96	2.75	0.98	

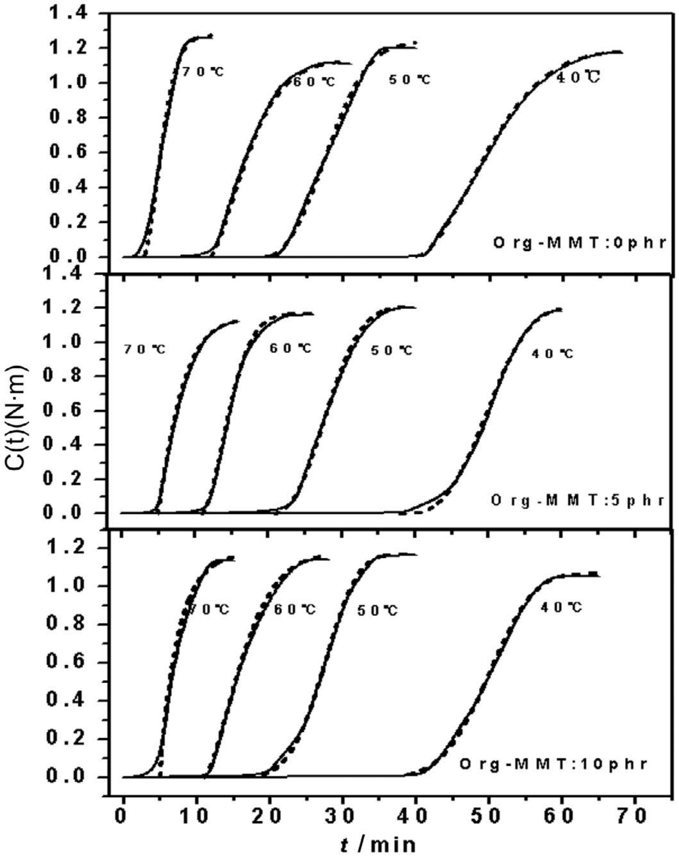

Fig. 4 Cure curve of epoxy resin/Org-MMT/DETA systems at various temperatures; — – experimental, --- – theoretical

to this theory, the physical or mechanical properties of the resin system during cure can be expressed as

$$\frac{G_\infty - G(t)}{G_\infty - G_0} = \exp\left[-\left(\frac{t}{\tau}\right)^{\beta}\right] \qquad (1)$$

where G_0 and G_∞ are the initial and final physical or mechanical properties during cure, respectively, $G(t)$ is the property at time t, τ is the time parameter (relaxation time) of the reaction system, and β represents the constant describing the width of the relaxation spectrum. In our experiment the mechanical property is torque. As seen from the isothermal cure curve in Fig. 4, G_0 is zero, the torque begins to appear only after the gel time t_g. Equation (1) describing the cure curve after t_g would be

$$\frac{G_\infty - G(t)}{G_\infty} = \exp\left(-\left[\left(\frac{t-t_g}{\tau}\right)^\beta\right]\right) \quad (2)$$

or

$$G(t)=G_\infty\{1-\exp[-t-t_g/\tau)^\beta]\} \quad (3)$$

Equation (3) describes the changes in torque of the resin system during cure in which t_g and G_∞ can be read directly from the experimental isothermal cure curve.

In order to obtain the relaxation time τ, let $t=t_g+\tau$; thus

$$G(t=t_g+\tau)=G_\infty(1-e^{-1})=0.63G_\infty \quad (4)$$

From a measurement of the time corresponding to $0.63G_\infty$ in the experimental cure curve, the relaxation time can be obtained from Eq. (4):

$$\tau=t-t_g$$

The relationship between the relaxation time τ and the cure temperature T is in accordance with Arrhenius equation [14]. Therefore, a straight line can be reached by plotting of $\ln\tau$ *vs.* $1/T$, and the τ_0 can be estimated from the intercept of the line as seen in Table 1. The reciprocal of τ_0 is the inflection on the rate of cure reaction of system. It is evident that the addition of Org-MMT leads to decrease the value of τ_0, that is, increase the value of $1/\tau_0$. Correspondingly, the addition of Org-MMT accelerates the rate of cure reaction, which may be the result of introducing of a new surface to the reaction system.

Having determined τ, Eq. (3) is reduced to an equation with a single parameter only. A non-linear regression is used to fit Eq. (3) to all experimental cure curves. The values of β at various curing temperatures or Org-MMT contents can be determined using the line of best fit. With this β value, the torque $G(t)$ for any time, i.e., the theoretically predicted value, can be calculated according to the Eq. (3) provided that the gel time t_g and the relaxation time τ are already known. The theoretical cure curves are also plotted in Fig. 4 as dotted lines. The theoretical prediction shows good agreement with the experimental curves for various curing temperatures.

Analysis of cure curve after gel time by Avrami method

The relative degree of cure, α at time t can be calculated according to cure curve as following

$$\alpha=\frac{G(t)}{G_\infty} \quad (5)$$

and the isothermal cure α curves can be changed into the relationship between degree of cure α and curing time $(t-t_g)$ after gel point, as shown in Fig. 5. Assuming that the isothermal cure process is similar with the isothermal crystallization process, the isothermal cure process can be analyzed using Avrami equation [18]:

$$\alpha=1-\exp[-k(t-t_g)^n] \tag{6}$$

or

$$\ln[-\ln(1-\alpha)]=n\ln(t-t_g)+\ln k \tag{7}$$

where t is the cure time; t_g the gel time; n the Avrami exponent that is a reflection of nucleation and growth mechanism; and k a temperature dependent kinetic constant.

Plots of $\ln[-\ln(1-\alpha)]$ *vs*. $\ln(t-t_g)$ for the data obtained on the cure process of epoxy/Org-MMT/diethylenetriamine are shown in Fig. 6. The results treated by Avrami equation are reported in Table 2. The good linearity indicates the validity of illustrat-

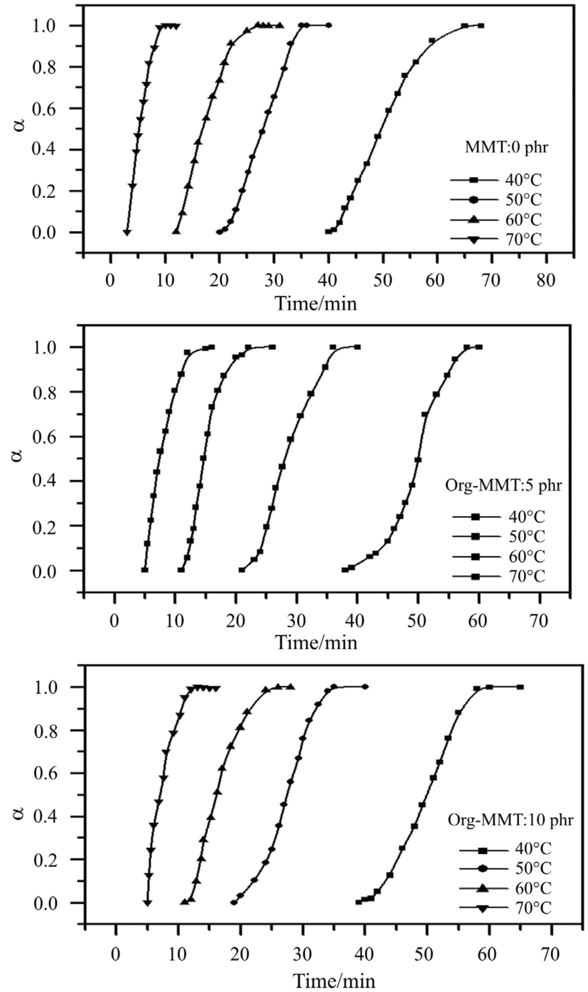

Fig. 5 Degree of cure as a function of cure time for epoxy resin/Org-MMT/DETA systems at different temperatures and filler contents

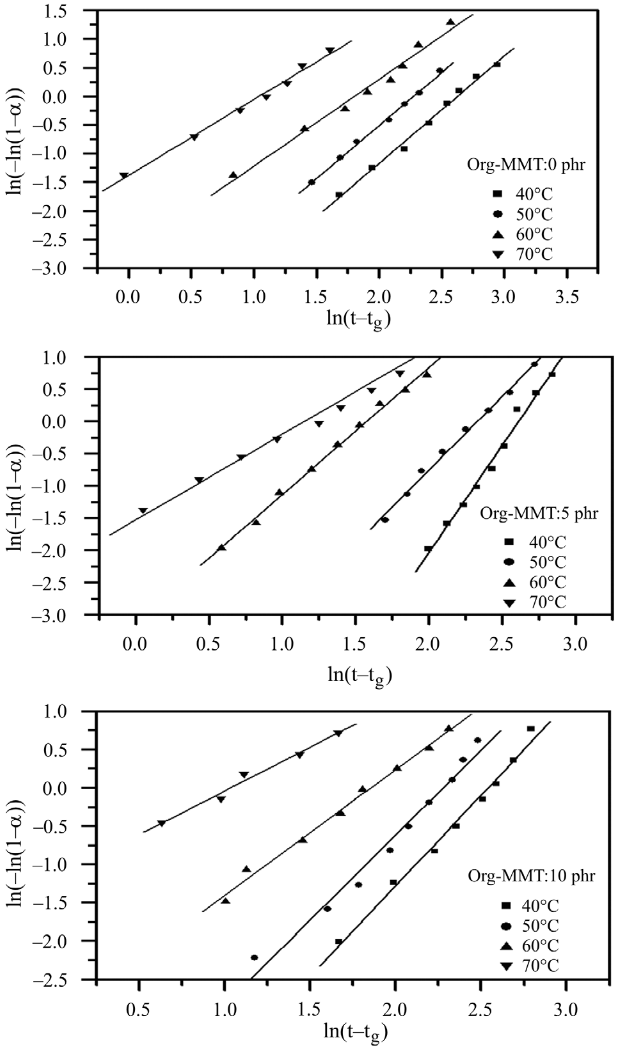

Fig. 6 Avrami plots of ln[–ln(1–α)] *vs*. ln(t–t_g) of epoxy resin/Org-MMT/DETA systems

ing the cure process after t_g by Avrami equation. Meanwhile, we found that the values of kinetic constant k decreased as the cure temperature increased, that is, the higher temperature, the faster cure reaction rate, which is good agreement with the general rule of chemical reaction [19]. The values of the Avrami exponent n depend on the cure temperatures for epoxy/Org-MMT/diethylenetriamine systems. At the lower temperature (<60°C) the n values were close to a constant 2 and decreased to ~1.5 as the temperature increased. Similar results are obtained in epoxy resin/diethylenetriamine systems without Org-MMT. Since the n value provides the qualitative information on the reaction mechanism, we may conclude that the cure reaction

Table 2 Values of isothermal curing process of epoxy/Org-MMT/DETA systems

Org-MMT (phr)	T/°C	t_g/min	$t_{1/2}$/min	k	n	E_a^*/ kJ mol^{-1}	E_a^{**}/ kJ mol^{-1}
0	40	40.01	16.82	$7.40 \cdot 10^{-3}$	1.87	73.5	44.9
	50	19.83	8.40	$1.49 \cdot 10^{-2}$	1.85		
	60	11.93	5.17	$6.53 \cdot 10^{-2}$	1.51		
	70	3.01	2.28	0.253	1.32		
5	40	37.65	12.36	$1.66 \cdot 10^{-4}$	3.33	59.6	45.7
	50	19.52	8.59	$4.86 \cdot 10^{-3}$	2.29		
	60	10.73	3.89	$4.47 \cdot 10^{-2}$	1.98		
	70	4.95	2.37	0.217	1.33		
10	40	38.70	11.32	$2.46 \cdot 10^{-3}$	2.36	59.9	43.7
	50	19.04	8.41	$6.39 \cdot 10^{-3}$	2.22		
	60	10.91	5.00	$4.76 \cdot 10^{-2}$	1.64		
	70	4.96	2.13	0.306	1.44		

*Activation energy before gelation point
**Activation energy after gelation point

has less of a mass transfer limitation in the low cure temperatures. The similar result was observed for a zeolite-filled epoxy system by Lu [20].

The half-time of cure, $t_{1/2}$, experimental and theoretical data by equation, $t_{1/2}=(\ln 2/k)^{1/n}$, compared closely in Table 2 for epoxy resin/Org-MMT/diethylenetriamine systems, confirming the ability of the Avrami model to represent isothermal cure process.

Apparent activation energy of resin system

According to Flory's gelation theory [21], the chemical conversion at the gel point of the resin system is constant and is not related to the reaction temperature and experimental conditions. As a result, the apparent activation energy of cure reaction E_a can be obtained from the gel time t_g

$$\ln t_g = C + E_a/RT \tag{8}$$

where T is the curing temperature (in K), R the gas constant, and C a constant. Figure 7 shows a plot of $\ln t_g$ *vs*. $1/T$ for various content of Org-MMT of 0, 5 and 10 phr. The apparent activation energy E_a can be calculated from the slope of the lines.

The activation energy can also be calculated through the Avrami method. An empirical approach can be used to describe the temperature dependence of kinetic constant k. Assuming that k is thermally activated [22]:

$$k^{1/n} = k_0 \exp(-E_a/RT) \tag{9}$$

where E_a is an activation energy associated with the cure process and k_0 is a pre-exponential constant, the logarithmic plots of $(1/n)\ln k$ as a function of $1/T$ are shown in Fig. 8 for epoxy resin/Org-MMT/diethylenetriamine systems. The good fitting linear straight lines allow to calculate the activation energy from the slope of the straight line.

The values of activation energy obtained by the above methods are reported in Table 2. For the epoxy resin/diethylenetriamine system, the value of activation energy is 73.5 and 44.9 kJ mol^{-1}, respectively. The addition of Org-MMT (i.e., 5 phr content of Org-MMT) to epoxy resin/diethylenetriamine systems leads to the activation energy of 59.6, 45.7 kJ mol^{-1}, respectively. Thus the addition of Org-MMT to epoxy resin/diethylenetriamine systems has a different effect on activation energy, dependent on whether the cure procedure (chemical control or diffusion control) is before or after the gelation point, that is, the addition of Org-MMT decreases the active energy before gelation point, but almost no activation energy change is found after gelation point, which the curing reaction is of diffusion control, for the cure procedure of epoxy resin/Org-MMT/DETA systems.

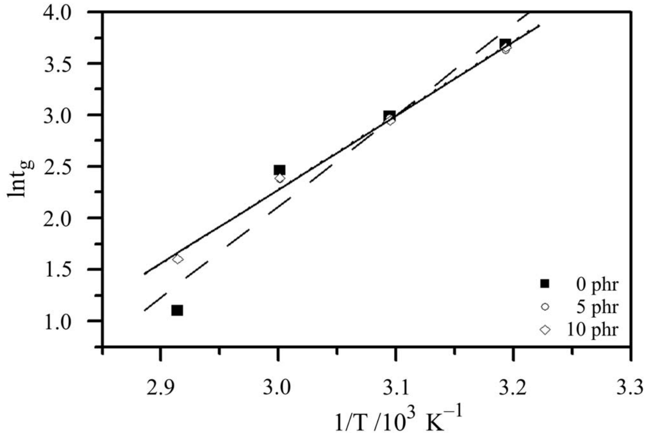

Fig. 7 Plots of lnt_g *vs.* $1/T$ of epoxy/Org-MMT/DETA systems

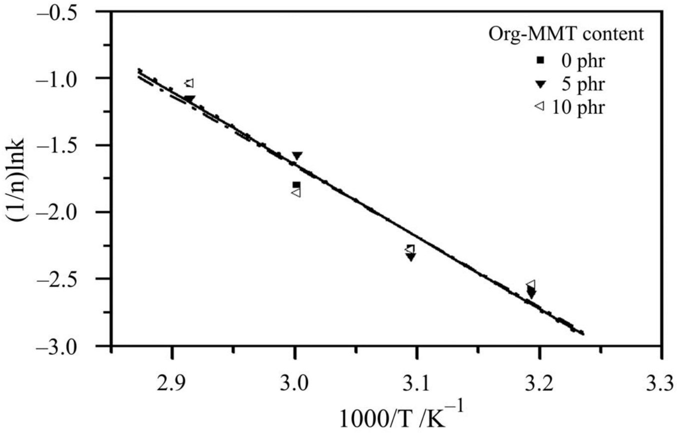

Fig. 8 Plots of $1/n\ln k$ *vs.* $1/T$ of epoxy resin/Org-MMT/DETA systems

Conclusions

The isothermal cure behavior of epoxy resin/organo-montmorillonite/diethylenetriamine intercalated nanocomposites was investigated by dynamic torsional vibration method in resin curemeter. The Flory's gelation theory, non-equilibrium thermodynamic fluctuation theory and Avrami equation have been used to predict the gel time t_g and the cure behavior of epoxy resin/organo-montmorillonite/diethylenetriamine systems at various cure temperatures and organo-montmorillonite loadings. The theoretical prediction is in good agreement with the experimental results obtained by dynamic torsional vibration method. The addition of organo-montmorillonite reduces the gel time t_g (when the cure temperature is lower than 60°C) and increases the rate of curing reaction, the value of k, and half-time of cure after gelation point $t_{1/2}$ decreases with the increasing of cure temperature, and the value of n is ~2 when the cure temperature is lower than 60°C, but it drops to ~1.5 above 60°C, and the addition of organo-montmorillonite decreases the apparent activation energy of the cure reaction before gelation point, but has no considerable effect on the apparent activation energy of the cure reaction after gelation point. Compared to the cure process of epoxy resin/diethylenetriamine in the presence or absence of organo-montmorillonite, no special curing process is required for the formation of epoxy resin/organo-montmorillonite/diethylenetriamine intercalated nanocomposite.

References

1 O. Becker, Y. Cheng, R. Varley and G. Simon, Macromolecules, 36 (2003) 1616.
2 J. Hlich, R. Thomann and R. Ihaupt, Macromolecules, 36 (2003) 7205.
3 X. Kornmann, H. Lindberg and L. A. Berglund, Polymer, 42 (2001) 1303.
4 X. Kornmann, H. Lindberg and L. A. Berglund, Polymer, 42 (2001) 4493.
5 I. J. Chir, T. Thurn-Albrecht, H. C. Kim, T. P. Russell and J. Wang, Polymer, 42 (2001) 5947.
6 P. P. Messersmith and E. P. Giannelis, Chem. Mater., 6 (1994) 1719.
7 T. Lar and T. J. Pinnavaia, Mater., 6 (1994) 2216.
8 T. Lan, P. D. Kaviratna and T. J. Pinnavaia, Proc. ACS division Polym. Mater. Sci. Eng., 71 (1994) 528.
9 T. Lan, P. D. Kaviratna and T. J. Pinnavaia, Chem. Mater., 7 (1995) 2144.
10 G. C. Stevens, J. Appl. Polym. Sci., 26 (1981) 4279.
11 R. M. Vinnik and A. A. Roznyatovsky, J. Therm. Anal. Cal., 74 (2003) 29.
12 R. M. Vinnik and A. A. Roznyatovsky, J. Therm. Anal. Cal., 76 (2004) 285.
13 P. S. He and C. E. Li, J. Appl. Polym. Sci., 43 (1991) 1011.
14 P. S. He and C. E. Li, J. Mater. Sci., 24 (1989) 2951.
15 W. B. Xu and P. S. He, Chinese Appl. Chem., 18 (2001) 469.
16 H. S.-Y. Hsich, J. Mater. Sci., 13 (1978) 2560.
17 H. S.-Y. Hsich, J. Appl. Polym. Sci., 27 (1982) 3265.
18 S. L. Liu, T. S. Chung and A. Yamaguchi, J. Polym. Sci. Part B: Polym. Phys., 36 (1998) 1679.
19 J. Smiitzis, A. Stamboulis, D. Tsoros and N. Martakis, Polym. Int., 43 (1997) 380.
20 M. G. Lu, M. G. Shim and S. W. Kim, Polym. Eng. Sci., 39 (1999) 274.
21 P. J. Flory, Principles of Polymer Chemistry, Cornell University Press, New York 1953.
22 C. Peggy and H. Su-Don, Polymer, 27 (1986) 1183.